

## Study of in-medium effect on the pion-nucleon amplitude from analysis of pion-nucleus data within the microscopic optical potential

---

**V.K.Lukyanov\*, E.V.Zemlyanaya, E.I.Zhabitskaya, K.V.Lukyanov, M.V.Zhabitsky**

*Joint Institute for Nuclear Research, 141980 Dubna, Russia*

*E-mail: vlukyanov@jinr.ru*

Analysis is performed of calculations of the elastic scattering differential cross sections of pions on the  $^{28}\text{Si}$ ,  $^{40}\text{Ca}$ ,  $^{58}\text{Ni}$  and  $^{208}\text{Pb}$  nuclei at energies from 130 to 290 MeV basing on the microscopic optical potential (OP) constructed as an optical limit of a Glauber theory. Such an OP is defined by the corresponding target nucleus density distribution and by the pion-nucleon  $\pi N$  amplitude of scattering. The pion-nucleus cross sections are calculated by numerical solving the corresponding relativistic wave equation. The three (say, “in-medium”) parameters of the  $\pi N$  amplitude, the total cross section, the ratio of real to imaginary part of the forward  $\pi N$  amplitude, and the slope parameter, were obtained by fitting the calculated cross sections to the respective experimental data. A difference is discussed between the best-fit “in-medium” parameters and the “free” parameters of the  $\pi N$  scattering amplitudes known from the experimental data on scattering of pions on free nucleons.

*XXI International Baldin Seminar on High Energy Physics Problems,  
September 10-15, 2012  
JINR, Dubna, Russia*

---

\*Speaker.

## 1. Introduction

Analysis of the data on scattering of pions from nuclei in the framework of microscopic models provides a possibility to study in-medium effect on the pion-nucleon amplitude of scattering. Indeed, this is the case when pions interact with the nucleons in nuclei rather than with the free one. To consider this effect we utilize the pion-nucleus microscopic optical potential constructed in [1] and based on the so-called optical limit of the high-energy approximation (HEA) for scattering of particles on nuclei [2]. Such an OP is defined by the known functions of density distribution of a target nucleus and by the  $\pi N$  amplitude of scattering. The  $\pi N$  amplitude itself depends on three parameters having a particular physical meaning, namely, the total cross section  $\sigma$ , the ratio  $\alpha$  of real to imaginary part of the  $\pi N$  amplitude at forward scattering, and the slope parameter  $\beta$  which characterizes its dependence on the momentum transfer. This HEA OP is then utilized to solve numerically the relativistic wave equation and thus the problem of the trajectory distortion in the standard Glauber approach is resolved automatically. So, varying parameters of this OP one can adjust calculated differential cross sections to the respective experimental data and thus obtain the best fit set of parameters to compare them with those of the free  $\pi N$  amplitude. The aim of our study is an explanation of experimental data in the region of (3 3)-resonance energies and estimation of the “in-medium” effect on the elementary pion-nucleon amplitude of scattering.

## 2. Basic formulas

The HEA-based microscopic optical potential  $U = U^H + U_C$  consists of nuclear and Coulomb parts. The nuclear part is derived in [1] as follows:

$$U^H = -\sigma(\alpha + i) \cdot \frac{\hbar c \beta_c}{(2\pi)^2} \int_0^\infty dq q^2 j_0(qr) \rho(q) f_{\pi N}(q), \quad f_{\pi N}(q) = e^{-\frac{\beta q^2}{2}}, \quad (2.1)$$

Here  $\hbar c = 197.327 \text{ MeV} \cdot \text{fm}$ ,  $\beta_c = k/E$  is the relativistic velocity,  $j_0$  is the spherical Bessel function, and  $f_{\pi N}(q)$  – form factor of  $\pi N$ -scattering amplitude

$$F_{\pi N}(q) = \frac{k}{4\pi} \sigma [i + \alpha] \cdot f_{\pi N}(q). \quad (2.2)$$

The form factor  $\rho(q)$  of the density distribution of point nucleons in nuclei we will take in the explicit form known for symmetrized Fermi-function:

$$\rho_{SF}(r) = \rho_0 \frac{\sinh(R/a)}{\cosh(R/a) + \cosh(r/a)}, \quad \rho_0 = \frac{3A}{4\pi R^3} \left[ 1 + \left( \frac{\pi a}{R} \right)^2 \right]^{-1}, \quad (2.3)$$

$$\rho_{SF}(q) = -\rho_0 \frac{4\pi^2 a R}{q} \frac{\cos qR}{\sinh(\pi a q)} \left[ 1 - \left( \frac{\pi a}{R} \right) \coth(\pi a q) \tan(qR) \right]. \quad (2.4)$$

Parameters of radius  $R$  and diffuseness  $a$  are known from electron-nucleus scattering data. As to the Coulomb part of OP, we utilize it as done by the sharp sphere with the charge  $eZ$  and radius  $R_c = r_c A^{1/3}$ . The latter is taken so that to get the same mean squared radii of potentials for the charged sphere and that calculated as the folding integral of the two charge interaction and the respective nuclear density distribution.

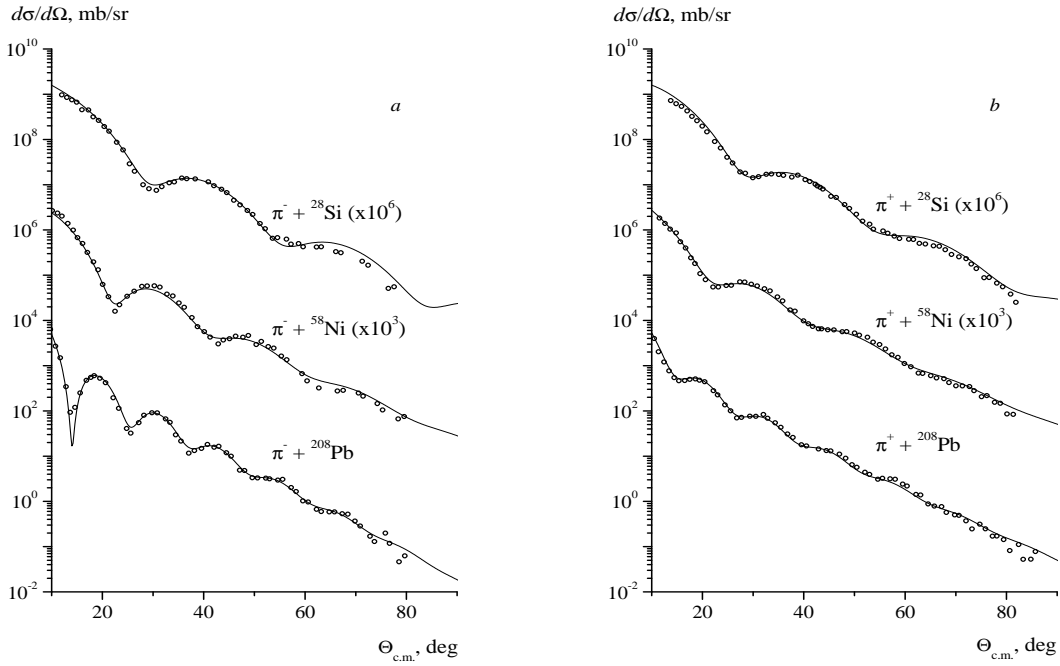


**Figure 1:** Comparison of the calculated pion-nucleus elastic scattering differential cross sections at  $T^{\text{lab}} = 291$  MeV with experimental data from [7]. The best-fit “in-medium” parameters  $\sigma$ ,  $\alpha$ , and  $\beta$  are given in the Table 1.

Using this OP the differential cross sections are calculated by solving the relativistic wave equation in analogy to that made in [3] for the kaon-nucleus scattering with the help of the standard DWUCK4 computer code [4]:

$$(\Delta + k^2) \psi(\vec{r}) = 2\bar{\mu}U(r)\psi(\vec{r}), \quad U(r) = U^H(r) + U_C(r). \quad (2.5)$$

Here  $k$  is relativistic momentum of pion in c.m. system

$$k = \frac{M_A k^{\text{lab}}}{\sqrt{(M_A + m_\pi)^2 + 2M_A T^{\text{lab}}}}, \quad k^{\text{lab}} = \sqrt{T^{\text{lab}}(T^{\text{lab}} + 2m_\pi)}, \quad (2.6)$$

$\bar{\mu} = EM_A/[E + M_A]$  – relativistic reduced mass,  $m_\pi$  and  $M_A$  – the pion and nucleus masses,  $E = \sqrt{k^2 + m_\pi^2}$  – total energy of  $\pi$ -meson in c.m. system,  $T^{\text{lab}}$  and  $k^{\text{lab}}$  – kinetic energy and momentum of pion in the laboratory system.

Our purpose is to fit the parameters  $\sigma$ ,  $\alpha$  and  $\beta$  of the  $\pi N$  scattering amplitude and thus to get the best agreement of the calculated  $\pi A$  differential cross sections with the respective experimental data. To this end we minimize the function

$$\chi^2 = f(\sigma, \alpha, \beta) = \sum_i \frac{(y_i - \hat{y}_i(\sigma, \alpha, \beta))^2}{s_i^2}. \quad (2.7)$$

where  $y_i = \log[\frac{d\sigma}{d\Omega}]_i$  and  $\hat{y}_i = \log[\frac{d\sigma}{d\Omega}(\sigma, \alpha, \beta)]_i$  are logarithms of, respectively, experimental and theoretical differential cross sections of elastic scattering;  $s_i$  is an error of  $i$ -th experimental point.

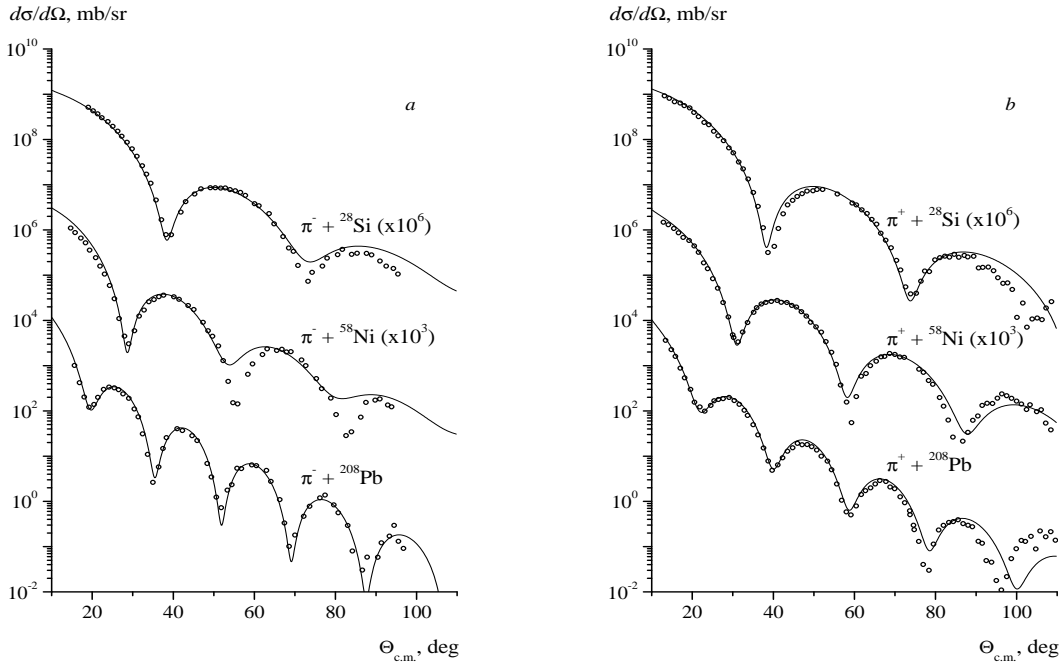


**Figure 2:** The same as in Figure 1 but for  $T^{lab} = 162$  MeV. The experimental data are from [8].

The fitting technique is based on the asynchronous differential evolution algorithm [5, 6] known as effective approach to obtain a global minimum of multi-parameter functions. One can note that if the value of the other minimum occurs closely to the global one then one should to invoke an additional (say, physical) information to select one of two sets of parameters.

### 3. Results and discussion

Figures 1–4 show the differential cross sections of elastic scattering of  $\pi^\pm$ -mesons on the target nuclei  $^{28}\text{Si}$ ,  $^{58}\text{Ni}$ ,  $^{40}\text{Ca}$ , and  $^{208}\text{Pb}$  at energies 130, 162, 180, 226, 230, and 291 MeV, in the region of the 33-resonance energy. The theoretical curves were calculated using the microscopic optical potentials presented in Section 2. All of them were compared with the respective experimental data [7]–[10] and the best-fit parameters  $\sigma$ ,  $\alpha$ , and  $\beta$  of the in-medium pion scattering amplitude and respective  $\chi^2$  values are given in the Table 1. In calculations were used the nuclear fermi-type density parameters for the point nucleon distributions, radius  $R$  and diffuseness  $a$ , as follows:  $R = 2.98$  fm and  $a = 0.533$  fm for  $^{28}\text{Si}$  [11];  $R = 4.08$  fm and  $a = 0.515$  fm for  $^{58}\text{Ni}$  [12];  $R = 3.593$  fm and  $a = 0.493$  fm for  $^{40}\text{Ca}$  [13];  $R = 6.654$  fm and  $a = 0.475$  fm for  $^{208}\text{Pb}$  [11].

It is seen that our results are in a reasonable agreement with experimental data. Some dissimilarity is observed only at large angles and can be explained by the fact that the standardly applied Gaussian form of  $\pi N$  form factor  $f_{\pi N}(q)$  is not exactly correct at comparably large angles of scattering and lower energies. Therefore the main contribution to the  $\chi^2$  values arises from disagreements at large angles. However the large amount of results show good agreement with experimental data

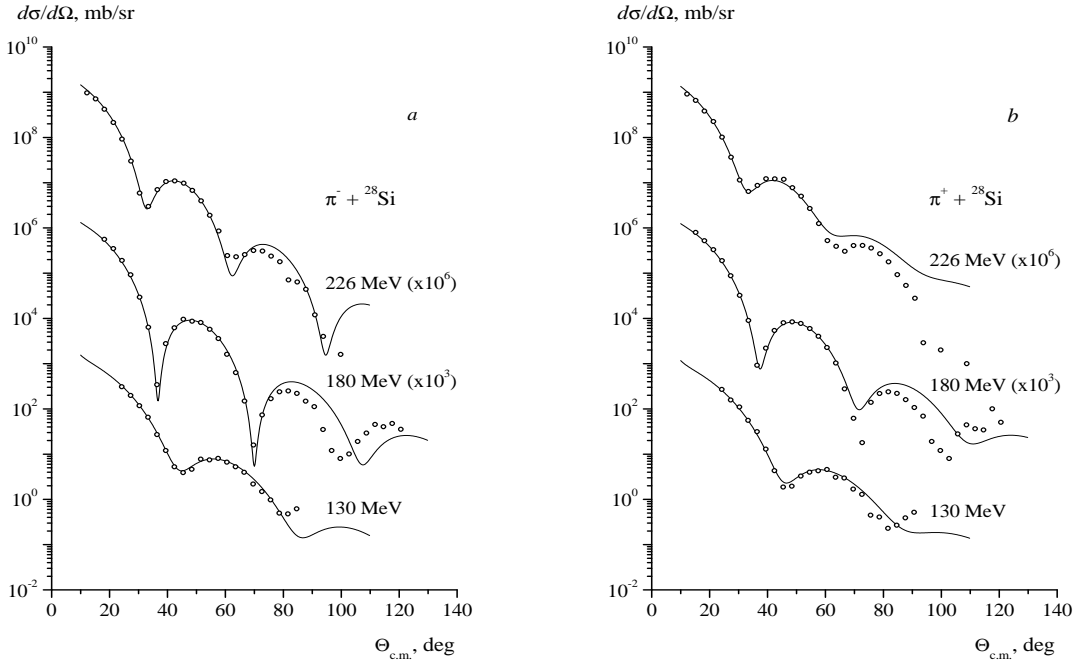


**Figure 3:** The same as in Figure 1 but for  $\pi$ -scattering on  $^{28}\text{Si}$  at  $T^{lab} = 130, 180, 226$  MeV. The experimental data are from [9].

and low  $\chi^2$  values enables one to do the certain conclusions on effects of the nuclear medium on the pion-nucleon interaction.

Figure 5 shows the averaged values  $X = (X_{\pi^+} + X_{\pi^-})/2$  where  $X$  means one of the parameters  $\sigma, \alpha, \beta$ . The comparisons are done of behaviors of the averaged "free"  $\pi^\pm N$ -scattering parameters [14, 15] with the best-fit "in-medium" parameters (we mark them by "eff") in their dependency on the collision energy  $T^{lab}$ .

Note, the bell-like forms of  $\sigma^{free}$  and  $\sigma^{eff}(T^{lab})$  have maximum at the same  $T^{lab}$ . The dark gray (blue) domain of in-medium  $\sigma^{eff}$  is located below the light gray (yellow)  $\sigma^{free}$  region in about 30%. This means that the "in-medium"  $\pi^\pm N$ -interaction becomes weaker as compared to that for "free"  $\pi^\pm N$ -scattering. It might be due to the Pauli-blocking effect, when incident pions interact with nucleons bounded in nuclear shells.

"In-medium"  $\alpha^{eff}(T^{lab})$  behavior indicates that the real part of the forward scattering  $\pi N$  amplitude retains to be positive at energies higher than the maximum of the 33-resonance energy  $T^{lab} > T_{res}^{lab} \simeq 170$  MeV while the  $\alpha^{free}$  changes the sign in this region. This means that when scattering in nuclear matter, the refraction of pions increases as compared to the "free" scattering, and with the follow increase of the energy it becomes the same as for the free pions. It is seen in the figure for  $\alpha$ , where the dark gray (blue) and light gray (yellow) regions become closer at  $T^{lab} > 250$  MeV.

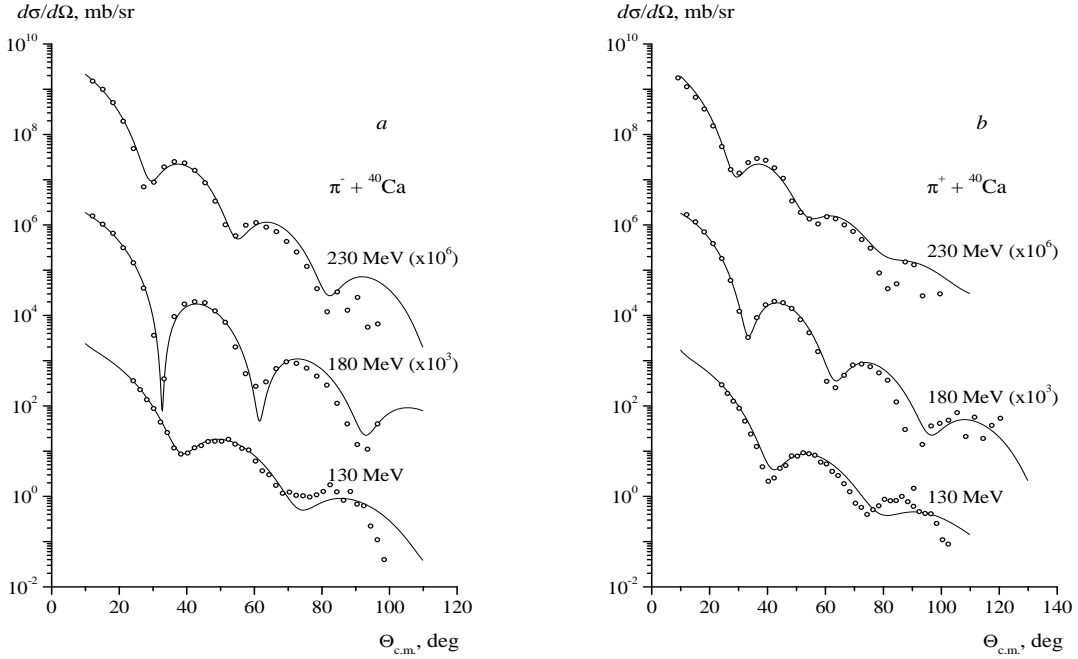


**Figure 4:** The same as in Figure 1 but for  $\pi$ -scattering on  $^{40}\text{Ca}$  at  $T^{lab} = 130, 180, 230$  MeV. Experimental data are from [10].

#### 4. Summary

- We shown that the HEA-based three-parametric microscopic OP provides a reasonable agreement with experimental data of the pion-nucleus elastic scattering differential cross sections on the nuclei  $^{28}\text{Si}$ ,  $^{58}\text{Ni}$ ,  $^{40}\text{Ca}$  and  $^{208}\text{Pb}$  at intermediate energies between 130 and 290 MeV in the region of angles of scattering up to 80 degrees.
- In all the cases it was gained that the nuclear medium has a pronounced effect on the the pion-nucleon amplitude of scattering in the region of the 33-resonance energies. As a result the energy dependence of all three parameters of the in-medium  $\pi N$ -amplitude differs noticeably from their behavior when scattering of pions on free nucleons.
- So, comparisons of  $\sigma^{free}$  and  $\sigma^{eff}$  show that the  $\pi N$ -interaction in nuclear matter is weaker than in the case of free  $\pi N$  collisions that can be caused by the Pauli blocking effect.
- Behavior of parameter  $\alpha^{eff}$  indicates that the refraction of pions in nuclear matter is larger as compared to  $\alpha^{free}$  at energies  $T^{lab} \geq T_{res}^{lab} \simeq 170$ .MeV, and then at larger energies it goes down and becomes comparable in values to  $\alpha^{free}$ .
- The decrease of the in-medium slope parameter  $\beta^{eff}$  in comparison to the free one  $\beta^{free}$  means that effective *rms* radius of the  $\pi N$ -system in nuclear medium becomes less than in the pion collisions with free nucleons.

**Table 1:** The best-fit parameters  $\sigma$ ,  $\alpha$ ,  $\beta$  and corresponding  $\chi^2/k$  quantities where  $k$  is the number of experimental points.

| reaction                    | $T^{lab}$ , Mev | $\chi^2/k$ | $\sigma$ , fm <sup>2</sup> | $\alpha$         | $\beta$ , fm <sup>2</sup> |
|-----------------------------|-----------------|------------|----------------------------|------------------|---------------------------|
| $\pi^- + {}^{28}\text{Si}$  | 130             | 2.4        | $7.02 \pm 0.18$            | $0.88 \pm 0.02$  | $0.82 \pm 0.05$           |
| $\pi^+ + {}^{28}\text{Si}$  |                 | 5.5        | $9.60 \pm 0.13$            | $0.03 \pm 0.02$  | $0.83 \pm 0.04$           |
| $\pi^- + {}^{40}\text{Ca}$  | 130             | 4.0        | $6.99 \pm 0.08$            | $0.90 \pm 0.01$  | $0.86 \pm 0.03$           |
| $\pi^+ + {}^{40}\text{Ca}$  |                 | 13.0       | $8.62 \pm 0.09$            | $0.09 \pm 0.01$  | $0.74 \pm 0.02$           |
| $\pi^- + {}^{28}\text{Si}$  | 162             | 4.0        | $8.93 \pm 0.09$            | $0.58 \pm 0.01$  | $0.47 \pm 0.02$           |
| $\pi^+ + {}^{28}\text{Si}$  |                 | 4.01       | $10.24 \pm 0.05$           | $0.36 \pm 0.01$  | $0.59 \pm 0.01$           |
| $\pi^- + {}^{58}\text{Ni}$  | 162             | 10.12      | $10.83 \pm 0.11$           | $-0.16 \pm 0.01$ | $1.11 \pm 0.02$           |
| $\pi^+ + {}^{58}\text{Ni}$  |                 | 6.5        | $9.28 \pm 0.04$            | $+0.44 \pm 0.01$ | $0.75 \pm 0.01$           |
| $\pi^- + {}^{208}\text{Pb}$ | 162             | 3.7        | $9.66 \pm 0.10$            | $0.35 \pm 0.01$  | $1.03 \pm 0.02$           |
| $\pi^+ + {}^{208}\text{Pb}$ |                 | 10.5       | $6.65 \pm 0.03$            | $0.61 \pm 0.01$  | $1.08 \pm 0.01$           |
| $\pi^- + {}^{28}\text{Si}$  | 180             | 10.24      | $10.11 \pm 0.05$           | $0.33 \pm 0.01$  | $0.24 \pm 0.01$           |
| $\pi^+ + {}^{28}\text{Si}$  |                 | 10.83      | $10.36 \pm 0.06$           | $0.29 \pm 0.01$  | $0.31 \pm 0.01$           |
| $\pi^- + {}^{40}\text{Ca}$  |                 | 2.8        | $9.65 \pm 0.10$            | $0.23 \pm 0.02$  | $0.28 \pm 0.01$           |
| $\pi^+ + {}^{40}\text{Ca}$  |                 | 3.35       | $5.78 \pm 0.07$            | $1.08 \pm 0.02$  | $0.69 \pm 0.02$           |
| $\pi^- + {}^{28}\text{Si}$  | 226             | 17.8       | $9.48 \pm 0.06$            | $-0.21 \pm 0.01$ | $0.143 \pm 0.01$          |
| $\pi^+ + {}^{28}\text{Si}$  |                 | 26.9       | $5.87 \pm 0.005$           | $1.08 \pm 0.01$  | $0.420 \pm 0.01$          |
| $\pi^- + {}^{40}\text{Ca}$  | 230             | 5.98       | $5.28 \pm 0.08$            | $0.80 \pm 0.01$  | $0.240 \pm 0.02$          |
| $\pi^+ + {}^{40}\text{Ca}$  |                 | 7.91       | $9.14 \pm 0.19$            | $-0.11 \pm 0.02$ | $0.246 \pm 0.03$          |
| $\pi^- + {}^{28}\text{Si}$  | 291             | 6.08       | $5.14 \pm 0.11$            | $-0.80 \pm 0.02$ | $0.16 \pm 0.02$           |
| $\pi^+ + {}^{28}\text{Si}$  |                 | 4.9        | $5.36 \pm 0.14$            | $-0.79 \pm 0.02$ | $0.368 \pm 0.02$          |
| $\pi^- + {}^{58}\text{Ni}$  |                 | 3.8        | $4.79 \pm 0.09$            | $-0.85 \pm 0.02$ | $0.281 \pm 0.01$          |
| $\pi^+ + {}^{58}\text{Ni}$  |                 | 2.6        | $5.56 \pm 0.09$            | $-0.67 \pm 0.02$ | $0.365 \pm 0.01$          |
| $\pi^- + {}^{208}\text{Pb}$ |                 | 4.1        | $4.46 \pm 0.07$            | $-1.07 \pm 0.02$ | $0.673 \pm 0.02$          |
| $\pi^+ + {}^{208}\text{Pb}$ |                 | 2.7        | $5.56 \pm 0.14$            | $-0.46 \pm 0.01$ | $0.588 \pm 0.02$          |

- Applications of the asynchronous differential evolution method for fitting to the data showed that sometimes two closed minima situated and therefore it is desirable to be involved in analysis the other information on a process [16], say, the total cross sections or some polarization characteristics measured independently.
- We should note that the usage of isospin averaged parameters of  $\pi^\pm N$ -scattering amplitudes in the microscopic OP (2.1) is available for nuclei with the same numbers of protons and neutrons  $Z \simeq A - Z$  [17]. Hence the case of  $\pi$ -scattering on  ${}^{208}\text{Pb}$  with significant difference between numbers of protons and neutrons requires a special consideration.

## Acknowledgements

The work was partly supported by the Program “JINR – Bulgaria”. Authors E.V.Z. and K.V.L. thank the RFBR for the partial financial support under grant No. 12-01-00396a.

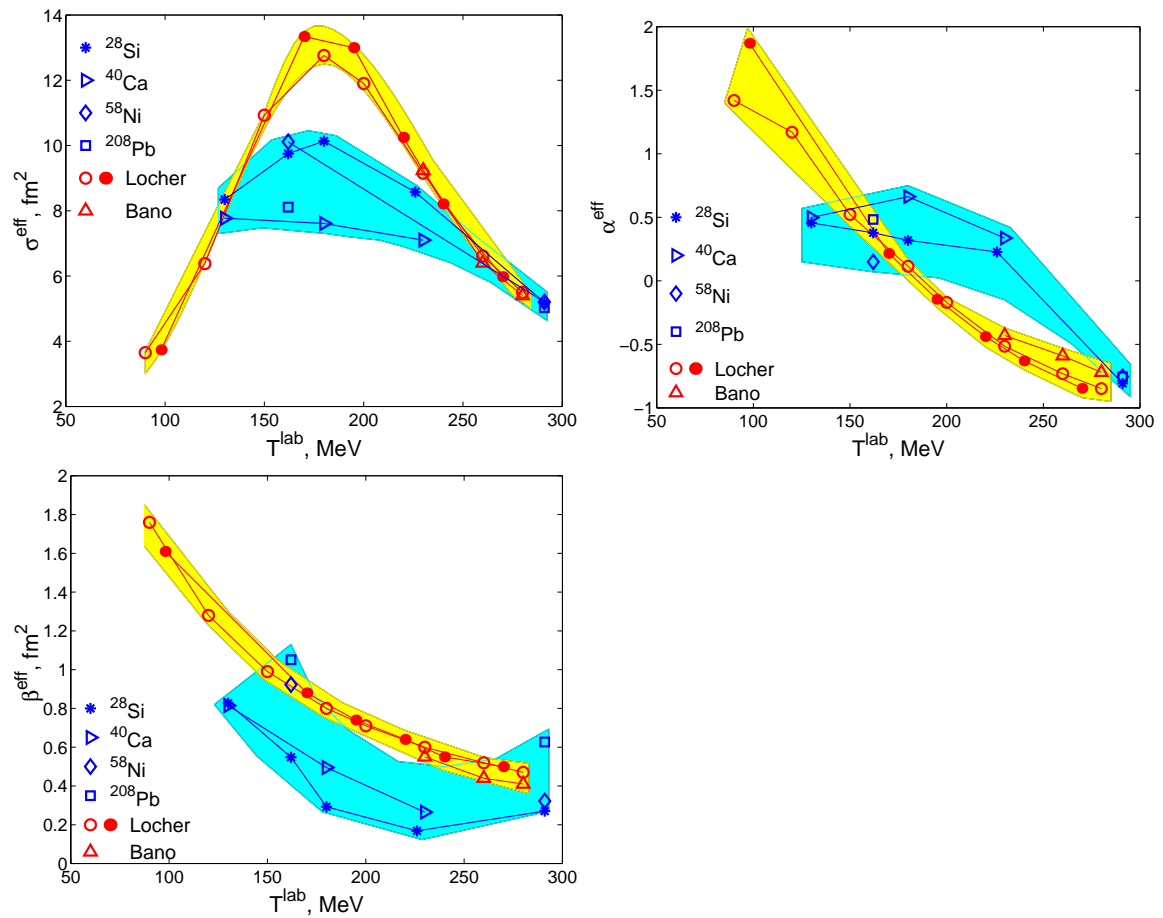


**Figure 5:** (Color online) Light gray (yellow): “free”  $\pi^\pm N$ -scattering parameters from [14] and [15]. Dark gray (blue): the best fit values  $X^{\text{eff}} = (X_{\pi^+} + X_{\pi^-})/2$ ;  $X = \sigma, \alpha, \beta$ .

## References

- [1] Lukyanov V.K., Zemlyanaya E.V., Lukyanov K.V. *Nucleus-nucleus scattering in the high-energy approximation and optical folding potential*. Phys. Atom. Nucl. **69** (2006) no.2, 240
- [2] Glauber R. J. *High-energy collision theory*. in Lectures in Theoretical Physics. Interscience, New York (1959)
- [3] Lukyanov V.K., Zemlyanaya E.V., Lukyanov K.V., Hanna K.M. *Microscopic  $K^+$ -nucleus optical potential and calculations of differential elastic scattering cross sections and total reaction cross sections*. Phys. Atom. Nucl. **73** (2010) no.8, 1443
- [4] Kunz P.D., Rost E. *Computational Nuclear Physics*, V.2, Eds. Langanke K. et al. Springer-Verlag (1993) 88
- [5] Zhabitskaya E.I., Zhabitsky M.V. *Asynchronous Differential Evolution*. Lecture Notes in Computer Sciences **7125** (2012) 328
- [6] Zhabitskaya E.I., Zhabitsky M.V., Zemlyanaya E.V., Lukyanov K.V. *Calculation of the parameters of microscopic optical potential for pion-nucleus elastic scattering by Asynchronous Differential Evolution algorithm* Computer Research and Modeling **4** (2012), no.3, 585

- [7] Geesaman D.F., Olmer C., Zeidman B., *et al.* Elastic and inelastic scattering of 291-Mev pions by  $^9\text{Be}$ ,  $\text{Si}$ ,  $^{58}\text{Ni}$ , and  $^{208}\text{Pb}$ . Phys. Rev. **C 23** (1981) 2635
- [8] Olmer C., *et al.* Elastic and inelastic scattering of 162 MeV pions on  $^{28}\text{Si}$ ,  $^{58}\text{Ni}$ , and  $^{208}\text{Pb}$ . Phys. Rev. **C 21**(1980) 254
- [9] B.M. Preedom *et al.* A systematic study of  $\pi^+$  and  $\pi^-$  inelastic scattering from  $^{28}\text{Si}$  in the region of the  $\pi N N(3,3)$  resonance. Nucl. Phys. **A 326** (1979) 385
- [10] Gretillat P. *et al.* Study of  $\pi^+$  and  $\pi^-$  elastic scattering from  $^{40}\text{Ca}$  and  $^{48}\text{Ca}$  in the region of the  $\pi N (3,3)$  resonance. Nucl. Phys. **A 364** (1981) 270
- [11] Patterson J.D., Peterson R.J. Empirical distributions of protons within nuclei. Nucl. Phys. **A 717** (2003) 235
- [12] Khoa D.T., Satchler G.R. Generalized folding model for elastic and inelastic nucleus-nucleus scattering using realistic density dependent nucleon-nucleon interaction. Nucl. Phys. **A 668** (2000) 3
- [13] Lukyanov V.K., Zemlyanaya E.V., Słowiński. Nucleus-nucleus reaction cross-sections calculated for realistic nuclear matter distributions within the Glauber-Sitenko approach. Phys. Atom. Nucl. **67** (2004) 1282
- [14] Locher M.P., Steinmann O., Straumann N. Why is the 33-resonance shifted in nuclei? Nucl. Phys. **B 27** (1971) 598
- [15] Bano N., Ahmad I. Medium-energy pion scattering and the  $\alpha$ -cluster description of  $^{12}\text{C}$ . J. Phys. **G 5** (1979) 39
- [16] Zemlyanaya E.V., Lukyanov V.K., Lukyanov K.V. , Zhabitskaya E.I., Zhabitsky M.V., Pion-Nucleus Microscopic Optical Potential at Intermediate Energies and In-Medium Effect on the Elementary  $\pi N$  Scattering Amplitude. arXiv:1210.1069v1 [nucl-th] (2012)
- [17] Lukyanov V.K., Zemlyanaya E.V., Lukyanov K.V., Ellithi A.Y., Abdel-Magead I.A.M., Slowinski B.. Analysis of the pion-nucleus elastic scattering using the microscopic optical potential. (To be published in Bulletin of the Russian Academy of Sciences. Physics)